

Risk-averse community resilience planning considering retrofit and insurance incentives

Tasnim Ibn Faiz, Kenneth W. Harrison & Zeinab Farahmandfar

To cite this article: Tasnim Ibn Faiz, Kenneth W. Harrison & Zeinab Farahmandfar (08 Feb 2026): Risk-averse community resilience planning considering retrofit and insurance incentives, Structure and Infrastructure Engineering, DOI: [10.1080/15732479.2026.2626405](https://doi.org/10.1080/15732479.2026.2626405)

To link to this article: <https://doi.org/10.1080/15732479.2026.2626405>



© 2026 The Author(s). Published by Informa UK Limited, trading as Taylor & Francis Group



[View supplementary material](#)



Published online: 08 Feb 2026.



[Submit your article to this journal](#)



Article views: 31



[View related articles](#)



[View Crossmark data](#)

Risk-averse community resilience planning considering retrofit and insurance incentives

Tasnim Ibn Faiz^{a,b} , Kenneth W. Harrison^c  and Zeinab Farahmandfar^b 

^aDepartment of Chemistry & Biochemistry, University of Maryland, College Park, Maryland, USA; ^bNIST Professional Research Experience Program (PREP), Engineering Laboratory, National Institute of Standards and Technology, Gaithersburg, Maryland, USA; ^cEngineering Laboratory, National Institute of Standards and Technology, Gaithersburg Maryland, USA

ABSTRACT

By taking proactive mitigation actions, a community can improve its resilience against natural disasters, which entails reducing vulnerability, minimising social impacts, and facilitating faster recovery. Mitigation planning for the built environment involves making appropriate decisions regarding strengthening interdependent utility network systems, adding redundancies, and retrofitting buildings. Due to the presence of numerous stakeholders with diverse socio-economic characteristics, different risk attitudes, and propensity to take voluntary actions, the planning problem is challenging, especially when the hazards, magnitudes, occurrence times, and impacts on the community's built environment and population are uncertain. An optimisation model, framed as a two-stage mean-risk stochastic programming model, was developed to address these challenges and support mitigation decisions. The optimisation model aims to minimise the costs and risks associated with hazards by integrating their impacts on the built environment and social functions. Under various incentive policies and risk preferences, the model helps generate decision alternatives and evaluate their effectiveness in achieving community resilience goals. A case study is presented using a community in Shelby County, Tennessee, subjected to earthquake hazards to demonstrate the model's capability to develop alternative mitigation strategies under varied risk preferences and incentive policies.

ARTICLE HISTORY

Received 17 September 2024
Revised 8 October 2025
Accepted 6 November 2025

KEYWORDS

Community resilience; incentive allocation; insurance; mitigation planning; optimization modelling; population dislocation; retrofit; risk-averse decision-making



1. Introduction


A community's resilience is reflected in the functional performance of its built environment and the state of its social and economic systems when faced with disruptions, whether caused by natural hazards and anthropogenic disasters (Summers et al., 2018). Structural damage and the loss of essential services (e.g., power, water) determine the functionality of critical infrastructure and buildings. Quantifying the effect of functionality loss in critical infrastructure on social systems is necessary to assess and improve community resilience. In their previous work (Faiz & Harrison, 2024), the authors of this paper formulated and tested an optimisation model to identify a suite of retrofit actions for critical infrastructure and residential buildings. The authors employed a risk-averse two-stage stochastic programming approach to identify resilience-enhancing decisions that consider the population dislocation and recovery delay as the consequences of functionality losses. In another work (Hu et al., 2023), loss in the labour force due to population dislocation and the economic impact were modelled using a computational general equilibrium model. On the other hand, social and economic disruptions, e.g., staff loss and increased travel time to hospitals and schools in the

aftermath of a hazard, are considered in Nofal et al., (2024). In this paper, although the proposed model limits its scope to population dislocation as the societal consequence, it incorporates more realism into the decision-making.

The underlying assumption in the authors' previous work and many other related research works is that homeowners of residential buildings will take the retrofit or any other mitigation actions prescribed by the decision-making model. Another assumption is that these actions can be implemented instantly to improve community resilience. However, retrofitting residential buildings, a voluntary mitigation measure, is not widespread, even in hazard-prone communities (Chiew et al., 2020), and the implementation of these actions is a gradual and slow-moving process. This is primarily due to high retrofit costs, long payback periods, and insufficient financial incentives (Egbelakin et al., 2017; Zhang et al., 2022). Therefore, community resilience planning involving residential buildings needs to consider homeowners' reservations about taking mitigation actions, the effects of incentives on overcoming them, and their incremental adoption.

The propensity to adopt voluntary retrofit can be impacted by federal, state, and local standards and policies. These standards and policies may include mandates for strengthening existing structures by retrofitting, upgrading structural

CONTACT Tasnim Ibn Faiz  tfaiz@umd.edu  University of Maryland, 8051 Regents Dr., College Park, MD 20742, USA.

 Supplemental data for this article can be accessed online at <https://doi.org/10.1080/15732479.2026.2626405>.

© 2026 The Author(s). Published by Informa UK Limited, trading as Taylor & Francis Group
This is an Open Access article distributed under the terms of the Creative Commons Attribution License (<http://creativecommons.org/licenses/by/4.0/>), which permits unrestricted use, distribution, and reproduction in any medium, provided the original work is properly cited. The terms on which this article has been published allow the posting of the Accepted Manuscript in a repository by the author(s) or with their consent.

standards, adopting disaster insurance, and incentivising community decision-makers and homeowners to take proactive actions. In this paper, retrofitting existing structures and adopting disaster insurance are considered as the available mitigation options, and the effect of mandates and incentive policies for motivating people to take these actions is studied.

Incentives, in different forms, including partial or full reimbursements, tax breaks, and low or zero-interest loans, can motivate building owners to undertake building retrofit measures. Absent any policies, voluntary retrofit depends on a building's location, age, structural properties, and also on building owners' socio-economic characteristics, prior hazard experience, and risk attitude (Zhang et al., 2022). However, the likelihood of taking a retrofit action increases if the associated cost is subsidised (Chiew et al., 2020; Jasour et al., 2018). An empirical study (Young et al., 2012) estimates that only 4% of residential buildings are voluntarily retrofitted against windstorms, whereas financial assistance or subsidies in the form of tax credits and extended loan periods can potentially increase this quantity up to 50%. Another study (Chiew et al., 2020) suggests that a \$1,000 increase in financial assistance leads to a 2% to 3% increase in the probability of retrofitting to protect against wind damage, whereas for elevating homes against flooding, the increase is 7%. California's Seismic Retrofit Incentive Program incentivizes homeowners to retrofit their homes (California Earthquake Authority (CEA), 2022). Some homeowners voluntarily participate in retrofitting programs only when the incentive is high; in some cases, if at least 75% of the retrofit costs are covered (Sattar, 2021). On a local scale, mandatory retrofitting laws can result in higher adoption rates. For example, seismic strengthening statutes in some jurisdictions in the state of California have resulted in increased retrofit actions for unreinforced masonry buildings (Seismic Safety Commission, 2006).

Hazard insurance for buildings is an alternative to retrofits for reducing the risk of hazard-induced losses. Hazard insurance reduces the risk of hazard-induced losses (Shan et al., 2017) for the building owner by transferring some or all financial risk to an insurance entity. The insuring body can be a for-profit organisation or an entity governed by the state or federal government, such as the National Flood Insurance Program (NFIP). Like retrofitting, hazard insurance is an underutilised risk management measure in the U.S. (Shan et al., 2017). The most significant factors influencing the rate of insurance adoption are annual premiums, deductibles, affordability, tenure length, proximity to a hazard source, and recent hazard experience (Jasour et al., 2018; National Academies of Sciences, Engineering, and Medicine, 2015).

Like retrofit grant programs, incentives can be used to increase adoption, in this case through discounted insurance premiums. Incentives can be disbursed directly to qualified homeowners or to a whole community. For example, under NFIP, based on credit points according to the Community Rating System, a community might be eligible for discounts on insurance premiums (National Academies of Sciences, Engineering, and Medicine, 2015). Hazard insurance and retrofitting are often treated as complementary actions

(Jasour et al., 2018). For example, the California Earthquake Authority's 'Brace + Bolt' program provides grants to adopt retrofit actions and allows discounts on insurance premiums for retrofitted buildings.

The primary contribution of this paper is the development of an optimisation model that prescribes mitigation decisions and their incremental implementation to improve community resilience under various risk preferences and differing incentive policies. The model can evaluate the effectiveness of various policies designed to incentivise mitigation actions. A mix of incentives—subsidies for retrofits and insurance premiums, and mandates, i.e., requirements that residential buildings be retrofitted to the minimum code by a given date, are considered. A case study is presented that illustrates the applicability of the proposed model in community resilience planning for a region vulnerable to earthquake hazards. The paper is organised as follows. In Section 2, the community resilience planning problem is discussed, followed by the formulation of the optimisation model. Section 3 presents a case study for simulated earthquake hazards and discusses the findings and insights from the numerical experiments. In Section 4, model limitations are discussed, and concluding remarks are provided.

2. Methodology

Built off of the authors' previous work (Faiz & Harrison, 2024), in this paper, the scope of the research problem is expanded to include several new aspects of community resilience planning. First, the adoption of hazard insurance is considered a voluntary mitigation action in addition to retrofitting for residential buildings. Second, incentive policies and mandates, which incentivise these voluntary actions, are considered. Third, a planning horizon and distinct time periods are introduced to account for the incremental disbursement of incentives and the gradual implementation of mitigation actions. Fourth, critical buildings, their retrofitting, potential functionality losses, and impact on emergency services are considered.

Various components of a community's built environment, connectivity, interdependencies, and relationship with human social systems before a hazard are visually represented in Figure 1. Utility networks and critical buildings are shown, which serve neighbourhoods, and the residential buildings within these neighbourhoods ultimately serve the population. It is assumed that the transportation network is unaffected by the hazard and remains functional, and therefore, it is not depicted in this figure. The components of the built environment take on different types (archetypes) and may be built to different codes and standards (codes).

Several sets are defined for different classes of nodes representing relevant entities in the community, as is done for different archetypes and structural codes. Focusing on utility networks, set V^U contains all utility network nodes, and sets B^U and S^U are defined for all archetypes and codes for utility nodes. Parameter Z_{ibs}^U denotes the initial number of structures with the archetype $b \in B^U$ and code $s \in S^U$ at node $i \in V^U$. These sets and parameters, along with those

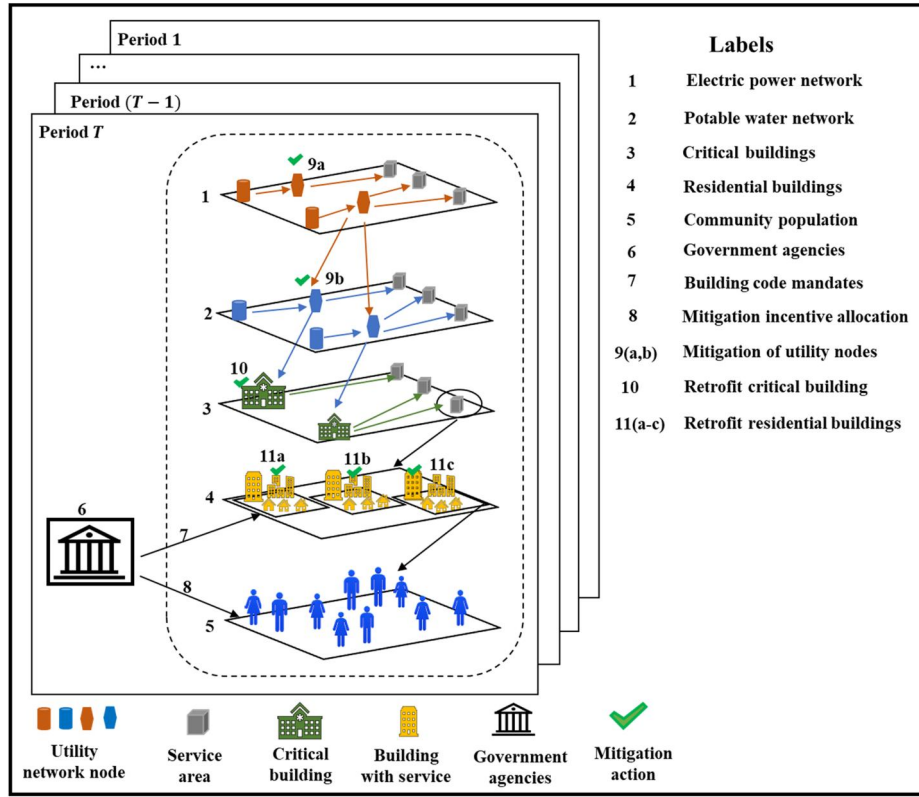


Figure 1. Simplified representation of a community in pre-hazard conditions.

Table 1. Definitions of sets related to nodes, arcs, archetypes, and structure codes.

Structure type	Set of:			Initial number of structures
	Nodes	Archetypes	Codes	
Utility network components	V^U	B^U	S^U	$\bar{Z}_{ibs}^U, \forall i \in V^U, b \in B^U, s \in S^U$
Critical buildings	V^C	B^C	S^C	$\bar{Z}_{ibs}^C, \forall i \in V^C, b \in B^C, s \in S^C$
Neighbourhoods	V^N	B^N	S^N	$\bar{Z}_{ibs}^N, \forall i \in V^N, b \in B^N, s \in S^N$

defined for critical buildings and neighbourhoods containing residential buildings are summarised in Table 1. The remaining sets and parameters are summarised in Appendices A.1 and A.2.

2.1. Mitigation actions for utility networks and critical buildings

To improve community resilience, during any period $\tau \in T$, represented by the cascading windows in Figure 1, mitigation actions can be taken, shown by green checkmarks. These actions include, for all structures, retrofitting, for all utility nodes and critical buildings, addition of storage (e.g., backup power, water), and adopting hazard insurance for residential buildings. Table 2 presents the set of variables related to the extent of retrofit actions for different structures (the remaining variable definitions are provided in Appendices A.3 and A.4). For example, variable n_{ibst}^{P-C} is the number of structures at the start of the period $\tau \in T$ at node $i \in V^C$ with archetype $b \in B^C$ and code $s \in S^C$, and $n_{ibst'}^{R-C}$ denotes the number of such structures upgraded to code $s' \in S^C$ during this period.

Table 2. Mitigation decision variables for structures.

Variable notation	Description				
	Number of structures at the beginning of period $\tau \in T$:				
	Node:	Archetype:	Code:		
n_{ibst}^{P-U}	$i \in V^U$	$b \in B^U$	$s \in S^U$		
n_{ibst}^{P-C}	$i \in V^C$	$b \in B^C$	$s \in S^C$		
n_{ibst}^{P-N}	$i \in V^N$	$b \in B^N$	$s \in S^N$		
Number of retrofitted structures during period $\tau \in T$:					
	Node:	Archetype:	From code:	To code:	Incentive:
$n_{ibst'}^{R-U}$	$i \in V^U$	$b \in B^U$	$s \in S^U$	$s' \in S^U$	–
$n_{ibst'}^{R-C}$	$i \in V^C$	$b \in B^C$	$s \in S^C$	$s' \in S^C$	–
$n_{ibst'}^{R1-N}$	$i \in V^N$	$b \in B^N$	$s \in S^N$	$s' \in S^N$	Yes
$n_{ibst'}^{R2-N}$	$i \in V^N$	$b \in B^N$	$s \in S^N$	$s' \in S^N$	No
Number of insured residential buildings during period $\tau \in T$:					
	Node:	Archetype:	From code:	Insurance:	Incentive:
n_{ibst}^{I1-N}	$i \in V^N$	$b \in B^N$	$s \in S^N$	$h \in H$	Yes
n_{ibst}^{I2-N}	$i \in V^N$	$b \in B^N$	$s \in S^N$	$h \in H$	No

Similar sets of variables, e.g., n_{ibst}^{P-U} and $n_{ibst'}^{R-U}$, are defined for utility network components. The constraints regulating these variables are governed by the constraints in Equations (A1)–(A6) of Appendices A.5 and A.6. The decision variables representing mitigation actions for residential buildings are discussed in Section 2.2. Mitigation actions for utility network components and critical buildings also include the addition of backup storage for power and water, which are

restricted by constraints in Equations (A7)–(A9) of Appendix A.7.

2.2. Mitigation actions for residential buildings

Two types of mitigation actions are considered for residential buildings: retrofitting and adoption of hazard insurance. The following subsections provide a detailed discussion of these two mitigation actions.

2.2.1. Retrofitting residential buildings

Retrofitting residential buildings is typically voluntary and requires a substantial investment from homeowners. It is assumed that only a small proportion of buildings ($\leq \bar{\delta}^R$ %) are retrofitted without financial incentive. However, by providing financial incentives, increased retrofit actions can be achieved (California Earthquake Authority (CEA), 2022; Chiew et al., 2020; Jasour et al., 2018; Young et al., 2012). To model the incentive disbursement and resulting retrofit actions, a set (G) of several incentive categories is considered. The binary variable $x_{ibsg\tau}^R, \forall i \in V^N, b \in B^N, s \in S^N, \tau \in T$ indicates whether the category $g \in G$ is selected for a group of buildings, and the variable $r_{ibsg\tau}^{R-SUB}$ denotes the disbursed incentive amount. If this amount is at least $\bar{\vartheta}^R$ % of the cost of a retrofit action, a fraction ($\leq \bar{\delta}^R$ %) of homeowners opt for retrofit. The variables $n_{ibss'\tau}^{R1-N}$ and $n_{ibss'\tau}^{R2-N}$ denote the number of buildings that take up the retrofit action of upgrading the code from $s \in S^N$ to $s' \in S^N$, with and without an incentive, respectively. The constraints in Equations (A10)–(A23) of Appendix A.8 enforce the incentive allocation decisions and retrofitting actions for residential buildings.

2.2.2. Adoption of hazard insurance

Like retrofit, the adoption of hazard insurance is usually voluntary. Several behavioural drivers influence the homeowners' adoption decision, including risk perception and prior hazard experience. Inclusion of these drivers and their impacts on homeowners' decisions, although it would bring more realism into the model, is not considered in the proposed model. Instead, the decisions by homeowners are assumed to be solely influenced by the presence of financial incentives, and higher incentives towards insurance premiums can result in more homeowners taking up insurance. It is assumed that at most $\bar{\delta}^I$ % of the residential homeowners adopt insurance without financial incentives, and the set G , the same used for the retrofit assistance, is considered as the set of incentive categories. The set H is defined as the set of all insurance products, where each $h \in H$ is characterised by the annual premium $\bar{\Lambda}_h$, deductible $\bar{\Delta}_h$, and coverage $\bar{\Psi}_h$.

The binary variable $x_{ibsg\tau}^I, \forall i \in V^N, b \in B^N, s \in S^N, \tau \in T$ indicates whether the category $g \in G$ is selected for the group of buildings and variable $r_{ibsg\tau}^{I-SUB}$ is the allocated incentive amount. If the amount exceeds at least $\bar{\vartheta}^I$ % of the annual premium, at most $\bar{\delta}^I$ % of the buildings in the group adopt insurance. The variables $n_{ibsh\tau}^{I1-N}$ and $n_{ibsh\tau}^{I2-N}$ denote

the number of buildings that take up insurance h with and without incentive, respectively. The variables $n_{ibsh\tau}^{UN}$ and $n_{ibsh\tau}^{IN}$ denote the number of total uninsured and insured buildings during each period, respectively. The constraints restricting assistance allocation and insurance adoption for residential buildings are presented in Equations (A24)–(A35) of Appendix A.9. The extent of mitigation actions, including retrofitting utility network components and critical buildings, and the amount of allocated financial incentives are restricted by the available budget. The budget limit is imposed by the constraint in Equation (A36) of Appendix A.10.

2.3. Variables and constraints associated with post-hazard conditions

Figure 2 represents a community's post-hazard status—panel A shows the immediate aftermath, and panel B depicts the recovery phase. Like in Figure 1, the transportation network is not depicted here as it is assumed that the transportation system remains fully functional. A finite probability space (Ω, Λ) is considered for uncertain hazard magnitude (i.e., loading $\tilde{L}_i, \forall i \in V^U \cup V^C \cup V^N$) and timing (\tilde{T}), where $\Omega = \{\omega^1, \omega^2, \dots, \omega^N\}$ is the set of scenarios with corresponding probabilities $\Lambda = \{\lambda^1, \lambda^2, \dots, \lambda^N\}$. The realisation of the random data $\xi(\omega)$ for a hazard event $\omega : \omega = \omega^1, \omega^2, \dots, \omega^N$, is denoted by $\xi^\omega = (\tilde{L}_{i\omega}, \tilde{T}_\omega)$ and occurs with a probability λ_ω . The hazard scenarios are represented by cascading windows with labels ranging from 'Scenario 1' to 'Scenario N'.

Given the loading and structural properties (archetype and code), the likelihood estimates of a structure being in or exceeding performance levels, i.e., damage states $f \in F$, are calculated using the fragility functions. These estimates are translated into binary parameters $\bar{W}_{ibsf\omega}^{S-U}, \bar{W}_{ibsf\omega}^{S-C}$, and $\bar{W}_{ibsf\omega}^{S-N}$ for utility network components, critical and residential buildings, respectively, to indicate whether a structure with archetype b and code s at node i falls into damage state $f \in F$ in scenario $\omega \in \Omega$ (see Appendix B.1). Damage may result in functionality losses at different structures shown by the red cross marks in Panel A of Figure 2. Functionality losses at utility network components lead to service outages, whereas the losses at critical buildings result in increased travel and waiting times to receive emergency services. The repair times for utility network components and critical buildings are governed by constraints in Equations (A37) and (A38), whereas Equations (A39)–(A42) dictate the time to restore service and recover functionality, and Equations (A43)–(A46) impose flow restrictions along the networks. These sets of constraints are presented in the Appendices A.11–A.13. The functional recovery of components is indicated by purple checkmarks in Panel B of Figure 2.

Structural damage may cause the residential buildings to lose functionality, which may lead to the temporary or permanent dislocation of the occupants if the population dislocation threshold (see Appendix B.2) is reached. The variables $n_{ibsf\omega}^{TD1}$ and $n_{ibsf\omega}^{PD1}$ denote the number of uninsured buildings experiencing temporary and permanent dislocation, respectively; similar two sets of variables for insured

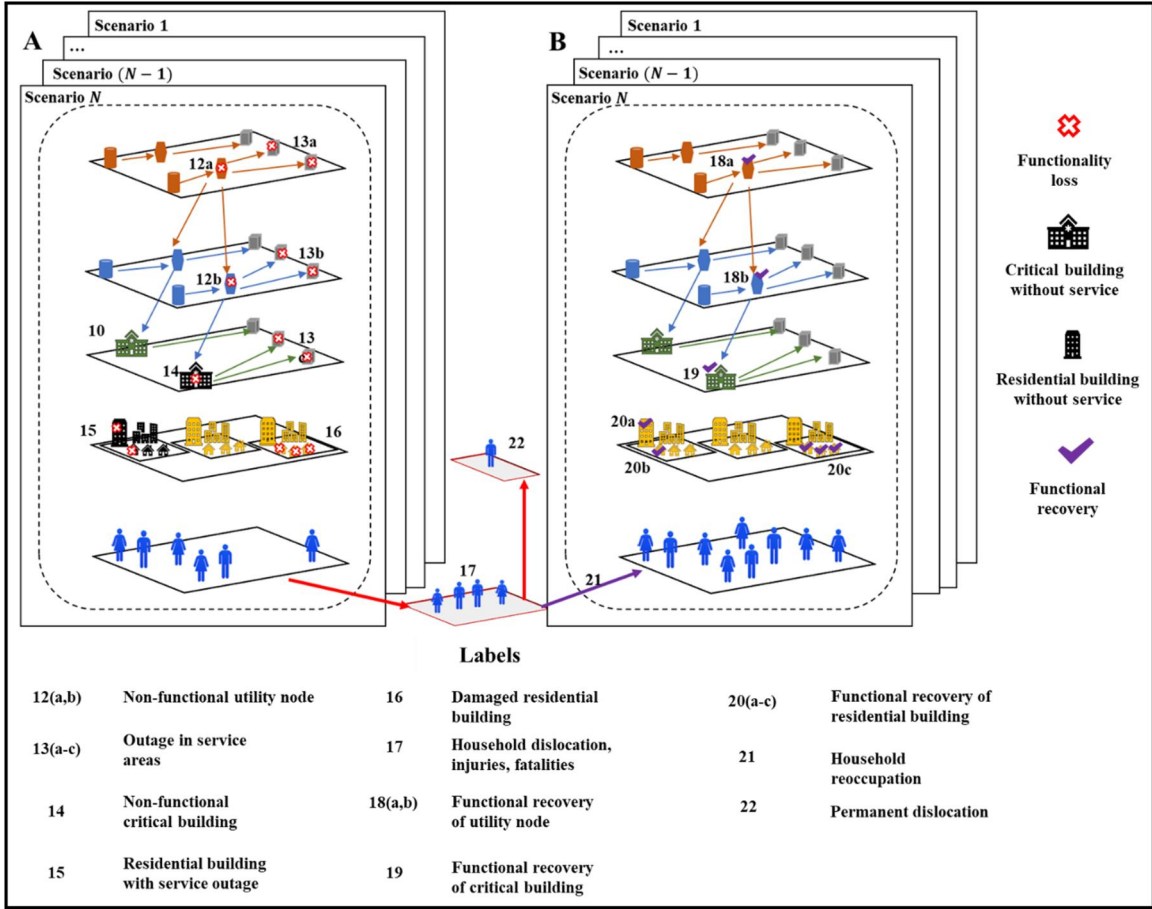


Figure 2. Simplified representation of a community in post-hazard conditions.

buildings are introduced as $n_{ibshf\omega}^{TD2}$ and $n_{ibshf\omega}^{PD2}$. The dislocation variables are governed by the constraints in Equations (A47) and (A48) of Appendix A.14. Damage in residential buildings can also result in fatalities and injuries to their occupants. The associated costs are estimated using the parameter Π_{jbf} denoting the proportion of occupants of buildings of archetype $\forall b \in B^N$ in a damage state $f \in F$ that fall into the injury severity level $j \in J$ (Federal Emergency Management Agency (FEMA), 2020).

2.4. Two-stage mean-risk stochastic programming model

The optimisation model proposed here aims to identify the optimal mitigation actions and incentive allocation decisions to facilitate achieving community resilience goals. The model is formulated as a mean-risk two-stage stochastic program, shown in Equations (1)–(7):

$$\text{Minimize} \left[(1 + \gamma)\theta^0 + \sum_{\omega \in \Omega} \lambda_{\omega} \theta_{\omega}^1 + \gamma\theta^2 \right] \quad (1)$$

Subject to:

$$\theta^0 = \sum_{\tau \in T} \left(\frac{1}{(1 + \rho)^{\tau\Delta}} \right) \left(\underbrace{\sum_{(i,b,s,\dot{s}) \in (V^U, B^U, S^U, S^U)} \bar{C}_{bss'}^{-1} n_{ibss'\tau}^{R-U}}_{\text{Utility retrofit costs}} \right)$$

$$\begin{aligned} & + \underbrace{\sum_{(i,b,s,\dot{s}) \in (V^C, B^C, S^C, S^C)} \bar{C}_{bss'}^2 n_{ibss'\tau}^{R-C}}_{\text{Critical building retrofit costs}} + \underbrace{\sum_{(i,b,s,\dot{s}) \in (V^N, B^N, S^N, S^N)} \bar{C}_{bss'}^3 (n_{ibss'\tau}^{R1-N} + n_{ibss'\tau}^{R2-N})}_{\text{Residential building retrofit costs}} \\ & - \underbrace{\sum_{(i,b,s,g) \in (V^N, B^N, S^N, G)} r_{ibsg\tau}^R \delta_g^R \bar{Z}_{ibs}^N}_{\text{Retrofit incentive allocated}} + \left(1 - \frac{1}{(1 + \rho)^\Delta} \right) \frac{1}{\rho} \\ & \left\{ \underbrace{\sum_{(i,b,s,h) \in (V^N, B^N, S^N, H)} \bar{C}_{ibsh}^4 (n_{ibsh\tau}^{I1-N} + n_{ibsh\tau}^{I2-N})}_{\text{Insurance adoption costs}} - \underbrace{\sum_{(i,b,s,g) \in (V^N, B^N, S^N, G)} r_{ibsg\tau}^R \delta_g^R \bar{Z}_{ibs}^N}_{\text{Insurance incentive allocated}} \right\} \\ & + \underbrace{\sum_{(k,i) \in (K, V_k^U)} \bar{C}_{ik}^5 e_{ik\tau}^{R-U}}_{\text{Utility storage cost}} \end{aligned} \quad (2)$$

$$\theta_{\omega}^1 = \underbrace{\sum_{(i,b,s,f) \in (V^U, B^U, S^U, F)} \bar{C}_{bsf}^6 n_{ibsf\omega}^{P-U} \bar{W}_{ibsf\omega}^{S-U}}_{\text{Utility recovery costs}} + \underbrace{\sum_{(i,b,s,f) \in (V^C, B^C, S^C, F)} \bar{C}_{bsf}^7 n_{ibsf\omega}^{P-C} \bar{W}_{ibsf\omega}^{S-C}}_{\text{Critical building retrofit costs}}$$

$$\begin{aligned}
& + \overbrace{\sum_{j \in V^U \cup V^C} \bar{C}_k^8 t_{j\omega}^R + \sum_{(i,b,s,k,j) \in (V^N, B^N, S^N, K \cup K', V^U \cup V^C)} \bar{C}_k^9 t_{j\omega}^R \bar{T}_{ijk}^M \bar{Z}_{ibs}^N \bar{U}_i \bar{P}}^{\text{Service outage costs}} \\
& + \overbrace{\sum_{(i,b,s,f) \in (V^N, B^N, S^N, F)} \left(\bar{C}_{bsf}^{10} + \bar{C}_{ib}^{11} \bar{A}_b + \bar{C}_{ib}^{13} \bar{D}_{bsf}^{R-N} \bar{A}_b \right) n_{ibsf\omega}^{TD1}}^{\text{Temporary dislocation costs from uninsured buildings}} \\
& + \overbrace{\sum_{(i,b,s,f,h) \in (V^N, B^N, S^N, F, H)} \left(\min\{\bar{C}_{bsf}^{10}, \bar{\Delta}_h\} + \max\{\bar{C}_{bsf}^{10} - \bar{\Psi}_h, 0\} + \bar{C}_{ib}^{11} \bar{A}_b + \bar{C}_{ib}^{13} \bar{D}_{bsf}^{R-N} \right) n_{ibsf\omega}^{TD2}}^{\text{Temporary dislocation costs from insured buildings}} \\
& + \overbrace{\sum_{(i,b,s,f) \in (V^N, B^N, S^N, F)} \bar{C}_{ib}^{12} n_{ibsf\omega}^{PD1} + \sum_{(i,b,s,f,h) \in (V^N, B^N, S^N, F, H)} \bar{C}_{ib}^{12} n_{ibsf\omega}^{PD2}}^{\text{Permanent dislocation costs from all residential buildings}} \\
& + \overbrace{\sum_{(i,b,s,f,j) \in (V^N, B^N, S^N, F, J)} \bar{C}_j^{14} \bar{W}_{ibsf\omega}^{S-N} \bar{U}_i \bar{P} \Pi_{jbf} n_{ibsf\omega}^{P-N}}^{\text{Injury and fatality costs}},
\end{aligned}$$

$$\omega \in \Omega \quad (3)$$

$$\theta^2 = v + \frac{1}{1-\alpha} \sum_{\omega \in \Omega} \lambda_\omega u_\omega \quad (4)$$

$$u_\omega \geq \theta_\omega^1 - v, \quad \omega \in \Omega \quad (5)$$

$$\text{Constraints (A1) – (A48)} \quad (6)$$

$$\text{Variable bounding constraints} \quad (7)$$

In the model's objective function shown in Equation (1), θ^0 represents the mitigation cost, θ_ω^1 is the cost in scenario $\omega \in \Omega$, and θ^2 represents the conditional value-at-risk (CVAR $_\alpha$) of the total cost at the confidence level α . The risk weight $\gamma \geq 0$ signifies the relative importance of risk compared to the expected cost. The constraints in Equations (2)–(4) dictate the computation of these cost components. The constraint (5) dictates the calculation of variable $u_\omega, \forall \omega \in \Omega$, i.e., the amount by which θ_ω^1 exceeds the value-at-risk, v . Constraints in Equations (A1)–(A48) of Appendices A.5–A.14 make up the system constraint shown in Equation (6). The variable bounding constraints are provided in Equation (7).

The objective function of the model is constructed using the mean-risk criterion (Ahmed, 2004; Noyan, 2012; Schultz & Tiedemann, 2006), and conditional value-at-risk as the risk measure (Rockafellar & Uryasev, 2000). The function minimises a weighted sum of expected cost and risk, which is essentially a scalarized version of the multi-objective optimisation problem with two competing objectives, expected cost and risk. By repeatedly solving the problem (1)–(7) with different values of $\gamma > 0$, the expected cost-risk efficient frontier of this multi-objective optimisation problem can be constructed.

3. Numerical results and discussion

This section presents numerical results from a case study to show the applicability of the proposed model in community

resilience planning. The AMPL modelling language (Fourer et al., 2003) is used to implement the model, and the FICO Xpress solver is used to solve the problem instances, yielding solutions that are within 1% of optimality. All experiments were conducted on a workstation equipped with a 16-core 2.60 GHz CPU and running a 64-bit Windows 10 operating system. A summary of the solver performance is provided in Appendix B.3.

3.1. Case study characteristics

The case study examines the community in Shelby County, Tennessee, which is located within the New Madrid Seismic Zone (NMSZ) and is therefore vulnerable to seismic hazards. The community comprises 284,547 residential buildings, distributed across 221 US Census tracts (neighbourhoods) and 36 critical buildings, including hospitals and fire stations. Fifteen archetypes and four structure codes are considered for buildings. Each structure in the utility service networks (59 in the electric power network and 49 in the potable water network) follows one of seven structure types and one of two standard codes. Five damage states are defined for all structures. Various cost, time, structural, and demographics parameter data are obtained from IN-CORE (Center of Excellence (COE), 2024) and the HAZUS earthquake manual (Federal Emergency Management Agency (FEMA), 2020).

Five financial incentive categories are considered, differing by the proportion of subsidised mitigation cost. To develop the categories, it is assumed that an additional 20% subsidisation of retrofit costs can increase retrofit adoption by at most 12.5%, whereas the same increase in insurance premiums can lead to at most a 10% increase in insurance adoption. Two hazard insurance products (H) are considered with \$150,000 and \$200,000 of loss coverage ($\bar{\Psi}_h$), 15% of the coverage as deductibles ($\bar{\Delta}_h$), and annual premiums ($\bar{\Lambda}_h$) of \$650 and \$750, respectively. The parameters $\bar{\delta}^R$ and $\bar{\delta}^I$ are set at 10%, which indicates that at most 10% of the buildings will adopt retrofit and insurance without assistance, respectively, whereas parameters $\bar{\mu}$ and $\bar{\gamma}$ are fixed at 75%, indicating that incentives can cover at most 75% of the total amount spent on retrofit and insurance.

The parameters for the population dislocation algorithm and restoration functions are taken from the literature (Center of Excellence (COE), 2024; Lin et al., 2008). The cost parameters related to utility and emergency service outages and the cost of injuries and fatalities are obtained from FEMA's benefit-cost analysis report (Federal Emergency Management Agency (FEMA), 2023a). To guide the model to prioritise more vulnerable neighbourhoods, social vulnerability indices of the neighbourhoods (e.g., SoVI) (Flanagan et al., 2011) are used as multipliers to obtain neighborhood-specific cost parameters related to dislocation. A 30-year planning horizon is considered, divided into six periods, each with 5-year intervals ($\Delta = 5$). The discount rate (ρ) is fixed at 0.07, and the budget (\bar{B}) is set at \$250 million.

3.2. Scenario generation procedure

One of the modelling assumptions is that a finite number of scenarios fully captures the uncertainty in the magnitude and timing of hazard events. To generate these scenarios, multiple earthquake events are considered, from which earthquake ground-motion intensity maps, i.e., hazard loadings, are generated using the Monte Carlo Simulation (MCS) technique (Crowley and Bommer, 2006). The magnitude-recurrence relationship (Gutenberg & Richter, 1944) is used to generate earthquake events of different magnitudes; the magnitude parameters are fed into a ground-motion model (Abrahamson et al., 2014) along with source-to-site distance and local geological conditions to predict the median ground-motion intensities, \overline{IM}_{ij} at site i for earthquake j . To account for prediction uncertainties, inter-event and intra-event residuals, i.e., the deviations between predicted and observed ground motions between earthquakes and within a single earthquake, respectively, are considered. The ground-motion model provides estimates for the standard deviations of both inter-event and intra-event residuals, enabling their normalisation.

The spatial correlations between inter-event and intra-event residuals at two sites are addressed using the method presented in Jayaram & Baker, (2009). Using the normalised residuals, the ground motion intensities or loadings of an earthquake scenario are obtained by following the method outlined in Jayaram & Baker (2010), as follows:

$$\ln IM_{ij} = \ln \overline{IM}_{ij} + \sigma_{ij}\varepsilon_{ij} + \pi_{ij}\eta_{ij} \quad (8)$$

where, IM_{ij} is the seismic intensity measure (e.g., peak ground acceleration, spectral acceleration) at the site i and for earthquake j , \overline{IM}_{ij} is the median ground-motion intensity, η_{ij} and ε_{ij} are the normalised inter-event and intra-event residuals, respectively, and π_{ij} and σ_{ij} are the standard deviations of inter-event and intra-event residuals, respectively.

Following the approach outlined above, six earthquake events are considered with exceedance probabilities of 2%, 5%, 10%, 20%, 50%, and 75% in 50 years (Cramer et al., 2009), followed by the calculation of the probabilities of exceedance in 5 years (since each period length $\Delta = 5$ years) for each. Next, five earthquake scenarios are constructed from each event: scenarios from the same event have the same ground motion intensity maps, i.e., loadings $\overline{L}_{i\omega}$, $\forall i \in V$ in peak ground acceleration (PGA) but different occurrence periods ($\overline{T}_{\omega} \in T$). The scenario occurrence probabilities (λ_{ω}) are determined by discretizing the exceedance curve.

3.3. Numerical results

For exposition purposes, the sources of uncertainty considered in all numerical experiments are limited to the earthquake magnitudes and the period of occurrence of hazard events. With minor modifications, the model could accommodate other sources of uncertainty, e.g., related to cost and repair time, by extending the scenario to include samples of

these parameters. This section examines and discusses the effects of risk preference and incentive policies on mitigation decisions aimed at reducing hazard-induced losses, costs, and population dislocation. The policies represent different combinations of financial incentives and mandates to encourage voluntary and mandatory retrofitting of residential buildings and the adoption of hazard insurance. Four incentive policies are considered in this study, which are as follows:

- **Policy 1:** Financial incentives are available for residential building retrofits and hazard insurance premiums. All buildings with the lowest code are mandated to be retrofitted by the end of the planning horizon.
- **Policy 2:** Financial incentives are available for residential building retrofits.
- **Policy 3:** Financial incentives are available for insurance premiums.
- **Policy 4:** No financial incentives are provided. All buildings with the lowest code are mandated to be retrofitted by the end of the planning horizon.

Among the above four policies, Policy 1 and Policy 4 include a mandate that requires all buildings with the lowest code to be retrofitted by the end of the planning horizon. This is enforced in the model by the constraint in Equation (A20) of Appendix A.8. Under both policies, the constraint in Equation (A19) of Appendix A.8 allows at most $\overline{\delta}^R$ of all buildings to be retrofitted in each period, without any incentive. This includes both mandated and non-mandated voluntary retrofits. If incentives are available (Policy 1), the allocated assistance can also be used towards the mandated retrofits. Otherwise, the building owners bear the total retrofitting cost (Policy 4).

It is of interest to see how varying degrees of risk aversion impact various metrics of interest under different incentive policies. The sensitivity analysis of the risk weight parameter γ provides a decision-maker with a suite of possible mitigation options for different risk aversions (Noyan, 2012; Xu et al., 2007). For a risk-neutral decision maker, γ is set to zero; in this case, the decision-maker chooses to minimise the expected cost only, disregarding the risk. On the other end of the spectrum, γ is set to ∞ , to minimise the risk without considering the expected cost; in this case, the decision-maker is extremely risk-averse. By varying γ within the range $(0, \infty)$, the entire spectrum of the expected cost-risk trade-off curve can be constructed and explored. In the presented analysis, the values for γ are varied within the range $[0, 1]$. The expected cost-risk trade-off curve for this range is shown in Appendix B.4. In practical applications, the decision-maker can iteratively explore the solutions obtained for different values of γ and select the one that yields the optimal trade-off between the expected cost and risk according to their risk aversion.

It should be noted that the insights from the sensitivity analysis and the cost-risk efficient frontiers only help a decision-maker in evaluating the trade-offs between different cost elements and between costs and risk for the chosen

ranges of the parameter γ , but the selection of the appropriate risk weight ultimately depends on the decision-maker's risk tolerance. A rich body of literature (Charness et al., 2013; Gore & Helgeson, 2024; Holt & Laury, 2002) has focused on developing approaches to elicit people's tolerances to risk and quantify them to calculate risk aversion parameters. A comparative analysis of the effects of different policies and risk preferences on the mitigation and expected scenario costs resulting from the four policies is presented in Figure 3a and b. In this analysis, the confidence level α is fixed at 0.8.

In Figure 3, it is observed that a risk-neutral approach results in the smallest mitigation cost and the highest expected scenario costs under all policies. The mitigation cost increases with the increase in γ values, whereas the expected scenario cost decreases. The largest increase in mitigation costs occurs under Policy 1, closely followed by that under Policy 2. Under both policies, incentives for retrofit actions are provided, and a significant increase in mitigation actions and costs results when the risk weight γ is increased, accompanied by a decrease in expected scenario costs. On the other hand, the effect of changing the risk weight on costs is comparatively insignificant under Policies 3 and 4, as these policies do not offer any incentives for retrofit actions.

The effects of various incentive policies on scenario costs and total cost distributions are investigated next. Figure 4 presents the tail-end of the total cost cumulative distribution functions to illustrate the very large costs observed in low-probability, high-consequence hazard scenarios. The distribution functions help compare the probabilities of total cost exceeding various cost thresholds under different incentive policies. The probabilities of incurring a total cost exceeding \$5 billion are nearly the same under Policies 1 and 2, i.e., policies with retrofit incentives, and both are smaller than the probabilities of exceedance under Policies 3 and 4. On the other hand, the probability of incurring a total cost greater than \$5 billion is higher under Policy 3 compared to the other three policies.

Figure 5a and b presents the variations in the two metrics of mitigation measures for residential buildings, e.g., the proportion of retrofitted and insured buildings under different policies and risk weights. In Figure 5a, the adoption of retrofit and insurance under Policy 2 follows very similar patterns as those given by Policy 1 with the change in risk

weight. Under both policies, 4% of the buildings are retrofitted when a risk-neutral approach is adopted, reaching 15% under both policies when $\gamma = 1$. Both policies provide financial incentives for retrofitting. However, unlike Policy 1, Policy 2 does not have a retrofit mandate. This indicates that even without a mandate, people are likely to retrofit buildings if financial assistance makes the action affordable. It is also seen in Figure 5a when financial incentives are available only for insurance premiums, as in Policy 3 and Policy 4, only 1% of the buildings are retrofitted under risk-neutral cases. Under these policies, the changes in the proportion of retrofitted buildings with increased risk weights are very small.

The effects of incentive policies and risk weights on insurance adoption actions are shown in Figure 5b. Under all four policies, the proportions of buildings with insurance are less than 0.05% when the values of γ are small (≤ 0.1). For larger values of γ , the proportion of insured buildings increases markedly compared to the risk-neutral case under Policy 1 and Policy 3. Both these policies offer incentives for insurance premiums. When $\gamma \geq 0.15$, the number of insured buildings increases 5.5 times under Policy 1, whereas under Policy 3, a 31-times increase is seen when $\gamma \geq 0.25$. On the other hand, under Policy 2 and Policy 4, the changes in insurance adoption are insignificant. It is evident from Figure 5 that the retrofit incentive is more effective in increasing the adoption of mitigation measures compared to the insurance incentive.

Population or household dislocation is one of the community resilience metrics of interest. The variation in household dislocation with the change in risk aversion under different policies is explored and shown in Figure 6, which

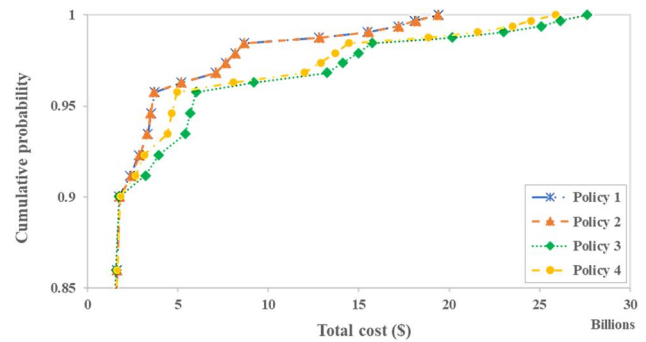


Figure 4. Cumulative distribution functions for the total cost for different incentive policies.

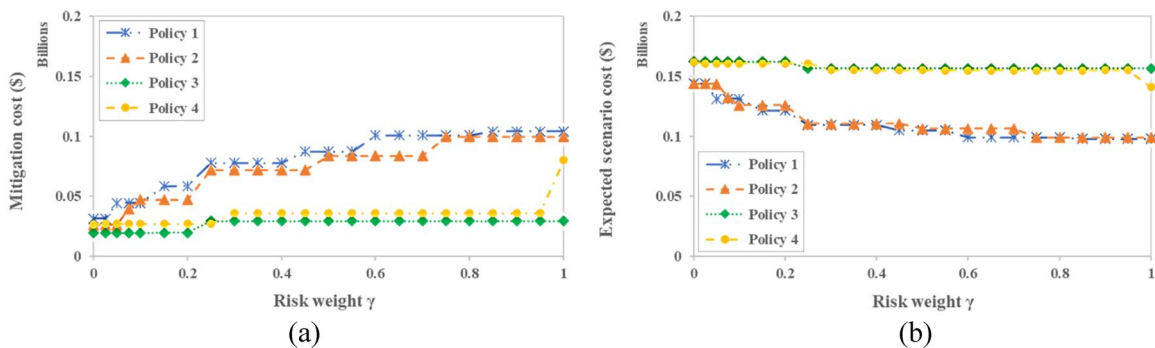


Figure 3. Effect of risk preference and incentive policies on: (a) mitigation cost and (b) expected scenario cost.

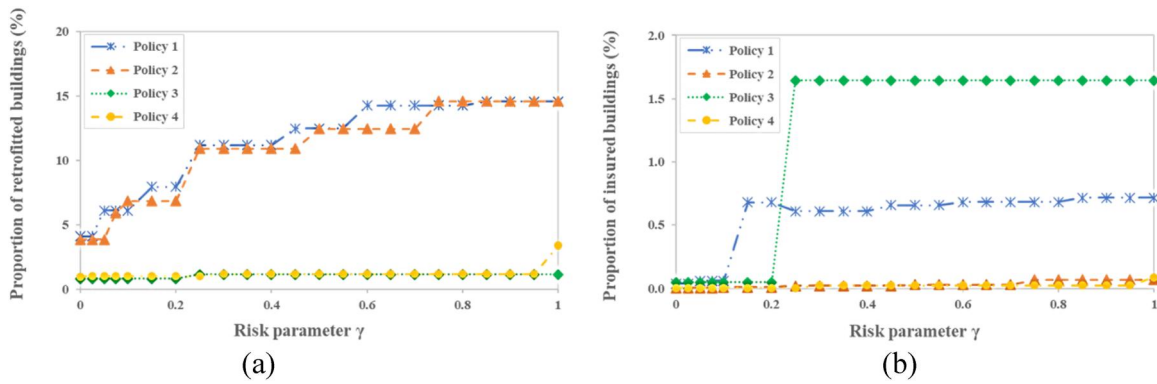


Figure 5. Effect of risk preference and incentive policies on: (a) proportion of retrofitted buildings and (b) proportion of insured buildings.

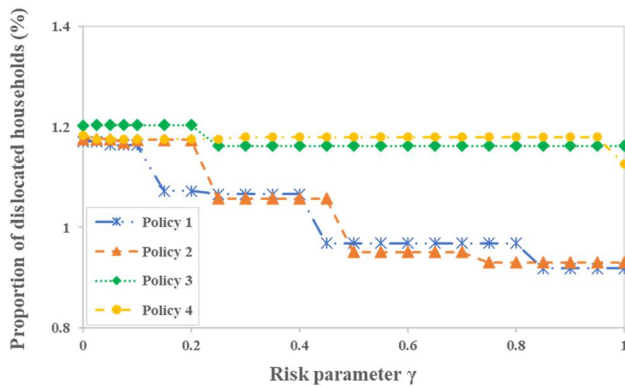


Figure 6. Effect of risk preference on the proportion of dislocated households for different incentive policies.

shows the variation for a representative scenario with a 5% exceedance probability in 50 years, occurring between years 20-25 of the 30-year planning horizon. The mitigation actions for residential buildings up to the time of hazard occurrence are shown in Figure 5.

In Figure 6, with the increase in γ values, decreasing trends in household dislocations are observed under Policy 1 and Policy 2; both these policies provide retrofit incentives. The other two policies, e.g., Policy 3 and Policy 4, which do not allow such assistance, result in markedly higher dislocation. The extent of household dislocation under the latter two policies also shows very low sensitivity to changing values of γ . In addition to various cost metrics, the proposed model's solutions provide optimal mitigation decisions and the resulting socio-economic consequences in various scenarios at different levels of granularity. The extent of mitigation measures for residential buildings and household dislocation across different neighbourhoods or census tracts is investigated, and an example is shown in Figure 7. Figure 7a presents the proportion of buildings that take retrofit actions in various census tracts, Figure 7b shows the insurance adoption, and Figure 7c presents the proportion of household dislocation in the representative hazard scenario.

4. Conclusions

Through mitigation measures, critical infrastructures and buildings in a community can become more resistant to

hazards and recover faster from damage. When developing mitigation plans for residential buildings, existing studies often overlook homeowners' reservations about taking voluntary mitigation measures, the impact of financial incentives on adoption decisions, and the gradual implementation of these measures. This study aims to incorporate more realism into decision-making by considering various incentive policies and their effects on voluntary mitigation actions and their incremental adoption. To that end, a decision-making model for community resilience planning has been developed, which takes the form of a mean-risk two-stage stochastic mixed integer linear program that considers costs and risks resulting from uncertain hazard events. The scope of this model is limited to a community's built environment, which includes utility service networks, critical and residential buildings, and the community's population. The model considers the costs and risks resulting from uncertain hazard events and utilises fragility functions and population dislocation models to translate hazard intensities into structural and societal consequences, incorporating them into the decision-making.

One limitation of this work is that it did not consider functionality losses in a community's transportation system, resulting in inaccessibility to hospitals, schools, and businesses, as well as delays in recovering utility services. A potential future direction of the research is the incorporation of the transportation network's post-hazard functionality losses and their impacts on service accessibility into the decision-making model. Another limitation is that the model considers population dislocation as the only societal consequence of the functionality losses in the residential buildings. However, population displacement has far-reaching consequences on a community, including the loss of employees and customers at businesses (Hu et al., 2023), teachers and students at schools (Nofal et al., 2024), and the loss of the local government's tax base (Zhu et al., 2025). The model can be improved by incorporating and updating empirical relationships between the functionalities of these institutions and population dislocation, which are continuously evolving in the area of community resilience research.

Finally, in modelling the retrofit and insurance adoption decisions, it is assumed that homeowners of buildings with the same characteristics are homogeneous and that the

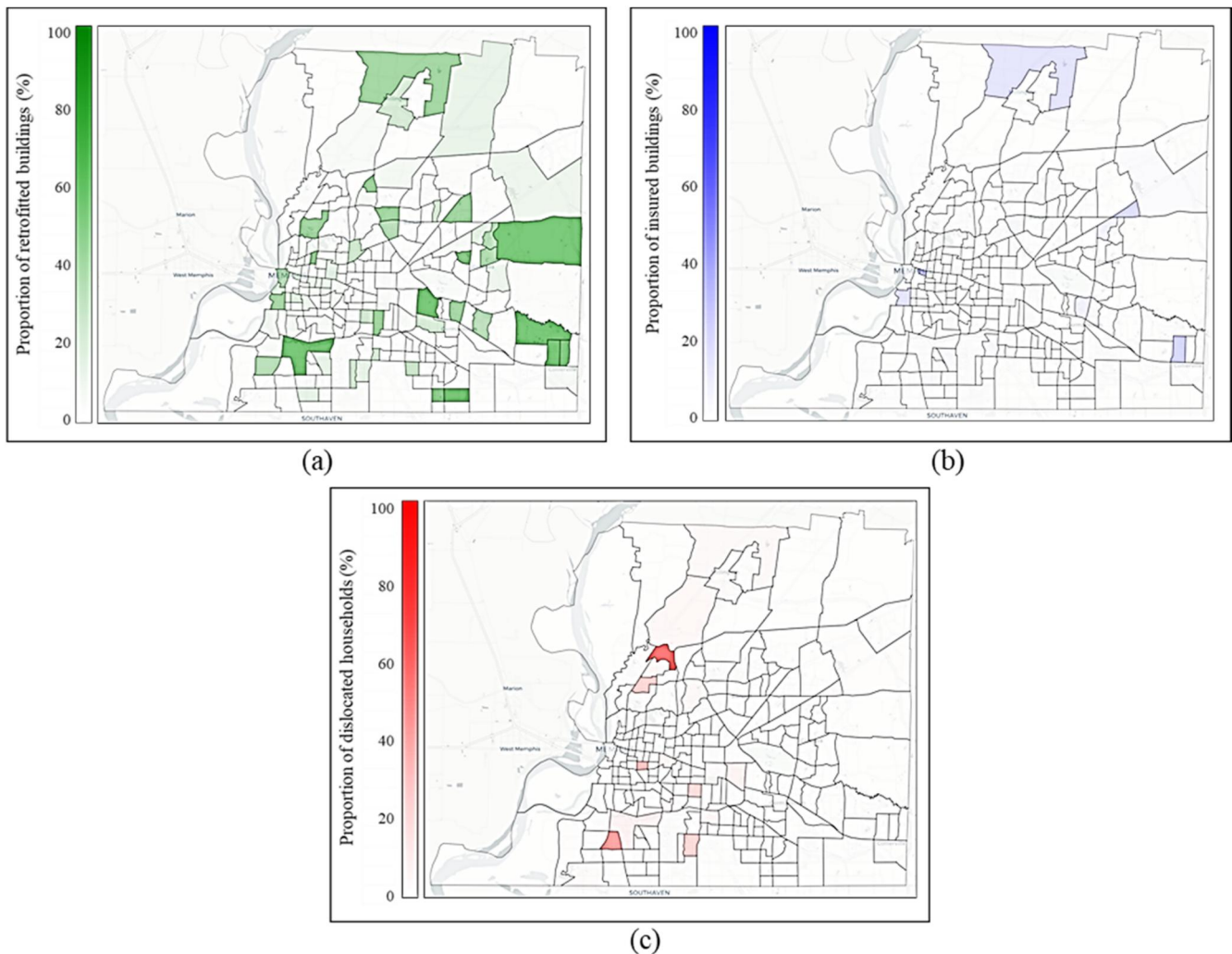


Figure 7. The proportion of residential buildings in various census tracts that: (a) are retrofitted, (b) are insured, (c) experience dislocation under policy 1 (© OpenStreetMap contributors).

extent of mitigation actions is driven by the financial incentives received. This oversimplifies the complex interaction of behavioural and economic drivers, such as risk perception, prior hazard experience, and affordability, that influence homeowners' decision-making. A possible future research extension direction could be the use of agent-based models to simulate decisions made by disparate homeowners and integrate them into the optimisation model.

ORCID

Tasnim Ibn Faiz  <http://orcid.org/0000-0003-1987-9863>

Kenneth W. Harrison  <http://orcid.org/0000-0002-6813-1854>

Zeinab Farahmandfar  <http://orcid.org/0000-0001-8912-0401>

Data availability statement

Data will be made available on request.

Disclosure statement

No potential conflict of interest was reported by the author(s).

References

- Abrahamson, N. A., Silva, W. J., & Kamai, R. (2014). Summary of the ASK14 ground motion relation for active crustal regions. *Earthquake Spectra*, 30(3), 1025–1055. <https://doi.org/10.1193/070913EQS198M>
- Ahmed, S. (2004). (with Humboldt-Universität Zu Berlin). *Mean-risk objectives in stochastic programming* (J. L. Higle, W. Römisch, & S. Sen, Eds.). Humboldt-Universität zu Berlin. Mathematisch-Naturwissenschaftliche Fakultät II, Institut für Mathematik. <https://doi.org/10.18452/8317>
- California Earthquake Authority (CEA). (2022). *Helping to mitigate Californians' seismic risks* (Nos. 2022-AB-100). <https://ssc.ca.gov/wp-content/uploads/sites/9/2022/12/2022-AB-100-Annual-Report-FINAL.pdf>
- Center of Excellence (COE). (2024). *Interdependent networked community resilience modeling environment (IN-CORE)* [Computer software]. <https://incore.nca.illinois.edu/>
- Charness, G., Gneezy, U., & Imas, A. (2013). Experimental methods: Eliciting risk preferences. *Journal of Economic Behavior & Organization*, 87, 43–51. <https://doi.org/10.1016/j.jebo.2012.12.023>
- Chiew, E., Davidson, R. A., Trainor, J. E., Nozick, L. K., & Kruse, J. L. (2020). The impact of grants on homeowner decisions to retrofit to reduce hurricane-induced wind and flood damage. *Weather, Climate, and Society*, 12(1), 31–46. <https://doi.org/10.1175/WCAS-D-18-0139.1>

- Cramer, C., Gomberg, J., Schweig, E., Waldron, B., & Tucker, K. (2009). *The Memphis, Shelby County, Tennessee, Seismic Hazard Maps*. (U.S. Geological Survey Open-File Report Nos. 04–1294). United States Geological Survey.
- Crowley, H., & Bommer, J. J. (2006). Modelling seismic hazard in earthquake loss models with spatially distributed exposure. *Bulletin of Earthquake Engineering*, 4(3), 249–273. <https://doi.org/10.1007/s10518-006-9009-y>
- Egbelakin, T., Wilkinson, S., Ingham, J., Potangaroa, R., & Sajoudi, M. (2017). Incentives and motivators for improving building resilience to earthquake disaster. *Natural Hazards Review*, 18(4), 04017008. [https://doi.org/10.1061/\(ASCE\)NH.1527-6996.0000249](https://doi.org/10.1061/(ASCE)NH.1527-6996.0000249)
- Faiz, T. I., & Harrison, K. W. (2024). A risk-averse stochastic optimization model for community resilience planning. *Socio-Economic Planning Sciences*, 92, 101835. <https://doi.org/10.1016/j.seps.2024.101835>
- Federal Emergency Management Agency (FEMA). (2020). *Hazus earthquake model technical manual*. https://www.fema.gov/sites/default/files/2020-10/fema_hazus_earthquake_technical_manual_4-2.pdf
- Federal Emergency Management Agency (FEMA). (2023). *Benefit-cost analysis sustainment and enhancements: Standard economic value methodology report* (No. 70FA6022F00000007). https://www.fema.gov/sites/default/files/documents/fema_standard-economic-values-methodology-report_2023.pdf
- Flanagan, B. E., Gregory, E. W., Hallisey, E. J., Heitgerd, J. L., & Lewis, B. (2011). A social vulnerability index for disaster management. *Journal of Homeland Security and Emergency Management*, 8(1), 0000102202154773551792. <https://doi.org/10.2202/1547-7355.1792>
- Fourer, R., Gay, D. M., & Kernighan, B. W. (2003). *AMPL: A modeling language for mathematical programming* (2nd ed.). Thomson/Brooks/Cole.
- Gore, C., & Helgeson, J. (2024). *Methods for elicitation of risk preferences and perceptions: An examination of individual and group risk preferences*. (No. NIST SP 1323; p. NIST SP 1323). National Institute of Standards and Technology (U.S.). <https://doi.org/10.6028/NIST.SP.1323>
- Gutenberg, B., & Richter, C. F. (1944). Frequency of earthquakes in California. *Bulletin of the Seismological Society of America*, 34(4), 185–188. <https://doi.org/10.1785/bssa0340040185>
- Holt, C. A., & Laury, S. K. (2002). Risk aversion and incentive effects. *American Economic Review*, 92(5), 1644–1655. <https://doi.org/10.1257/000282802762024700>
- Hu, Y., Cutler, H., & Mao, Y. (2023). Economic loss assessment for losses due to earthquake under an integrated building, lifeline, and transportation nexus: A spatial computable general equilibrium approach for Shelby County, TN. *Sustainability*, 15(11), 8610. <https://doi.org/10.3390/su15118610>
- Jasour, Z. Y., Davidson, R. A., Trainor, J. E., Kruse, J. L., & Nozick, L. K. (2018). Homeowner decisions to retrofit to reduce hurricane-induced wind and flood damage. *Journal of Infrastructure Systems*, 24(4), 04018026. [https://doi.org/10.1061/\(ASCE\)IS.1943-555X.0000452](https://doi.org/10.1061/(ASCE)IS.1943-555X.0000452)
- Jayaram, N., & Baker, J. W. (2009). Correlation model for spatially distributed ground-motion intensities. *Earthquake Engineering & Structural Dynamics*, 38(15), 1687–1708. <https://doi.org/10.1002/eqe.922>
- Jayaram, N., & Baker, J. W. (2010). Efficient sampling and data reduction techniques for probabilistic seismic lifeline risk assessment. *Earthquake Engineering & Structural Dynamics*, 39(10), 1109–1131. <https://doi.org/10.1002/eqe.988>
- Lin, Y.-S., Peacock, W. G., Lu, J.-C., & Zhang, Y. (2008). *Household dislocation algorithm 3: A logistic regression approach* (No. HRRC Reports: 08-05R). Hazard Reduction and Recovery Center, Texas A&M University. <https://www.arch.tamu.edu/app/uploads/2021/10/08-05R-Dislocation-Algorithm-34.pdf>
- National Academies of Sciences, Engineering, and Medicine. (2015). *Affordability of national flood insurance program premiums: report 1*. (p. 21709). National Academies Press. <https://doi.org/10.17226/21709>
- Nofal, O., Rosenheim, N., Kameshwar, S., Patil, J., Zhou, X., van de Lindt, J. W., Duenas-Osorio, L., Cha, E. J., Endrami, A., Sutley, E., Cutler, H., Lu, T., Wang, C., & Jeon, H. (2024). Community-level post-hazard functionality methodology for buildings exposed to floods. *Computer-Aided Civil and Infrastructure Engineering*, 39(8), 1099–1122. <https://doi.org/10.1111/mice.13135>
- Noyan, N. (2012). Risk-averse two-stage stochastic programming with an application to disaster management. *Computers & Operations Research*, 39(3), 541–559. <https://doi.org/10.1016/j.cor.2011.03.017>
- Rockafellar, R. T., & Uryasev, S. (2000). Optimization of conditional value-at-risk. *The Journal of Risk*, 2(3), 21–41. <https://doi.org/10.21314/JOR.2000.038>
- Sattar, S. (2021). *Recommended options for improving the built environment for post-earthquake reoccupancy and functional recovery time*. National Institute of Standards and Technology. <https://doi.org/10.6028/NIST.SP.1254>
- Schultz, R., & Tiedemann, S. (2006). Conditional value-at-risk in stochastic programs with mixed-integer recourse. *Mathematical Programming*, 105(2–3), 365–386. <https://doi.org/10.1007/s10107-005-0658-4>
- Seismic Safety Commission. (2006). *Status of the unreinforced masonry building law*. (2006 Progress Report to the Legislature No. SSC 2006-04). https://ssc.ca.gov/wp-content/uploads/sites/9/2020/08/cssc_2006_urm_report_final.pdf
- Shan, X., Peng, J., Kesete, Y., Gao, Y., Kruse, J., Davidson, R. A., & Nozick, L. K. (2017). Market insurance and self-insurance through retrofit: Analysis of hurricane risk in North Carolina. *ASCE-ASME Journal of Risk and Uncertainty in Engineering Systems, Part A: Civil Engineering*, 3(1), 04016012. <https://doi.org/10.1061/AJRUA6.0000887>
- Summers, J. K., Harwell, L. C., Smith, L. M., & Buck, K. D. (2018). Measuring community resilience to natural hazards: The Natural Hazard Resilience Screening Index (NaHRSI)—Development and Application to the United States. *GeoHealth*, 2(12), 372–394. <https://doi.org/10.1029/2018GH000160>
- Xu, N., Davidson, R. A., Nozick, L. K., & Dodo, A. (2007). The risk-return tradeoff in optimizing regional earthquake mitigation investment. *Structure and Infrastructure Engineering*, 3(2), 133–146. <https://doi.org/10.1080/15732470600591083>
- Young, M., Cleary, K., Ricker, B., Taylor, J., & Vaziri, P. (2012). Promoting mitigation in existing building populations using risk assessment models. *Journal of Wind Engineering and Industrial Aerodynamics*, 104–106, 285–292. <https://doi.org/10.1016/j.jweia.2012.05.001>
- Zhang, Y., Fung, J. F., Johnson, K. J., & Sattar, S. (2022). Motivators and impediments to seismic retrofit implementation for wood-frame soft-story buildings: A case study in California. *Earthquake Spectra: The Professional Journal of the Earthquake Engineering Research Institute*, 38(4), 2788–2812. <https://doi.org/10.1177/87552930221100844>
- Zhu, T., Avraam, C., & Baker, J. W. (2025). Macroeconomic models for predicting indirect impacts of disasters: A review. *Resilient Cities and Structures*, 4(3), 1–14. <https://doi.org/10.1016/j.rcns.2025.06.003>